nature food

Article

https://doi.org/10.1038/s43016-023-00910-x

A hidden demethylation pathway removes mercury from rice plants and mitigates mercury flux to food chains

Received: 2 February 2023

Accepted: 1 December 2023

Published online: 04 January 2024

Check for updates

Wenli Tang[1,25], Xu Bai[2,3,25], Yang Zhou[1,25], Christian Sonne[4,5] ✉, Mengjie Wu[1], Su Shiung Lam[6,7], Holger Hintelmann[8], Carl P. J. Mitchell[9], Alexander Johs[10], Baohua Gu[10], Luís Nunes[11], Cun Liu[12], Naixian Feng[13], Sihai Yang[14], Jörg Rinklebe[15], Yan Lin[16], Long Chen[17], Yanxu Zhang[18], Yanan Yang[1], Jiaqi Wang[1], Shouying Li[1], Qingru Wu[19,20], Yong Sik Ok[21], Diandou Xu[2], Hong Li[2], Xu-Xiang Zhang[1], Hongqiang Ren[1], Guibin Jiang[22], Zhifang Chai[2,23], Yuxi Gao[2] ✉, Jiating Zhao[2,24] ✉ & Huan Zhong[1] ✉

Dietary exposure to methylmercury (MeHg) causes irreversible damage to human cognition and is mitigated by photolysis and microbial demethylation of MeHg. Rice (*Oryza sativa* L.) has been identified as a major dietary source of MeHg. However, it remains unknown what drives the process within plants for MeHg to make its way from soils to rice and the subsequent human dietary exposure to Hg. Here we report a hidden pathway of MeHg demethylation independent of light and microorganisms in rice plants. This natural pathway is driven by reactive oxygen species generated in vivo, rapidly transforming MeHg to inorganic Hg and then eliminating Hg from plants as gaseous Hg°. MeHg concentrations in rice grains would increase by 2.4- to 4.7-fold without this pathway, which equates to intelligence quotient losses of 0.01–0.51 points per newborn in major rice-consuming countries, corresponding to annual economic losses of US$30.7–84.2 billion globally. This discovered pathway effectively removes Hg from human food webs, playing an important role in exposure mitigation and global Hg cycling.

Global concerns over the potent neurotoxin methylmercury (MeHg) have persisted for decades. After entering the biosphere, MeHg is efficiently transferred along food chains, magnifying its concentration up to ten-million-fold[1]. Even low-level dietary exposure to this ubiquitous toxin causes irreversible neurological damage in humans[2], reducing the intelligence quotient (IQ) of newborns[3] and their lifetime earnings. MeHg exposure has been reported to cause IQ decrements of 2,420,000 points, 600,000 points and 264,000 points per year in China, European countries and the United States, respectively, corresponding to yearly economic losses of approximately US$7.3, US$11 and US$5 billion[4–7]. Human exposure to MeHg is largely mitigated by its demethylation in natural environments, during which this potent neurotoxin is converted into less toxic inorganic forms before entering human food webs. Photolysis[8,9] and microbial demethylation[10–12] are the two widely recognized pathways of MeHg demethylation in the environment[13], effectively reducing the amount of MeHg available for bioaccumulation.

Despite decades of research and advances in understanding light- and microbe-mediated demethylation in surface water, soils and sediments[10,13–16], the role of plants in degrading MeHg remains unclear and is largely ignored. Although MeHg demethylation within rice has been inferred[17,18] even in soil–plant systems[19,20], it remains unknown what drives this process within plants which are key starting points for MeHg into human food webs. In particular, rice (*Oryza sativa* L.) has been

A full list of affiliations appears at the end of the paper. ✉e-mail: cs@ecos.au.dk; gaoyx@ihep.ac.cn; zhaojt@zju.edu.cn; zhonghuan@nju.edu.cn

https://doi.org/10.1038/s43016-023-00910-x

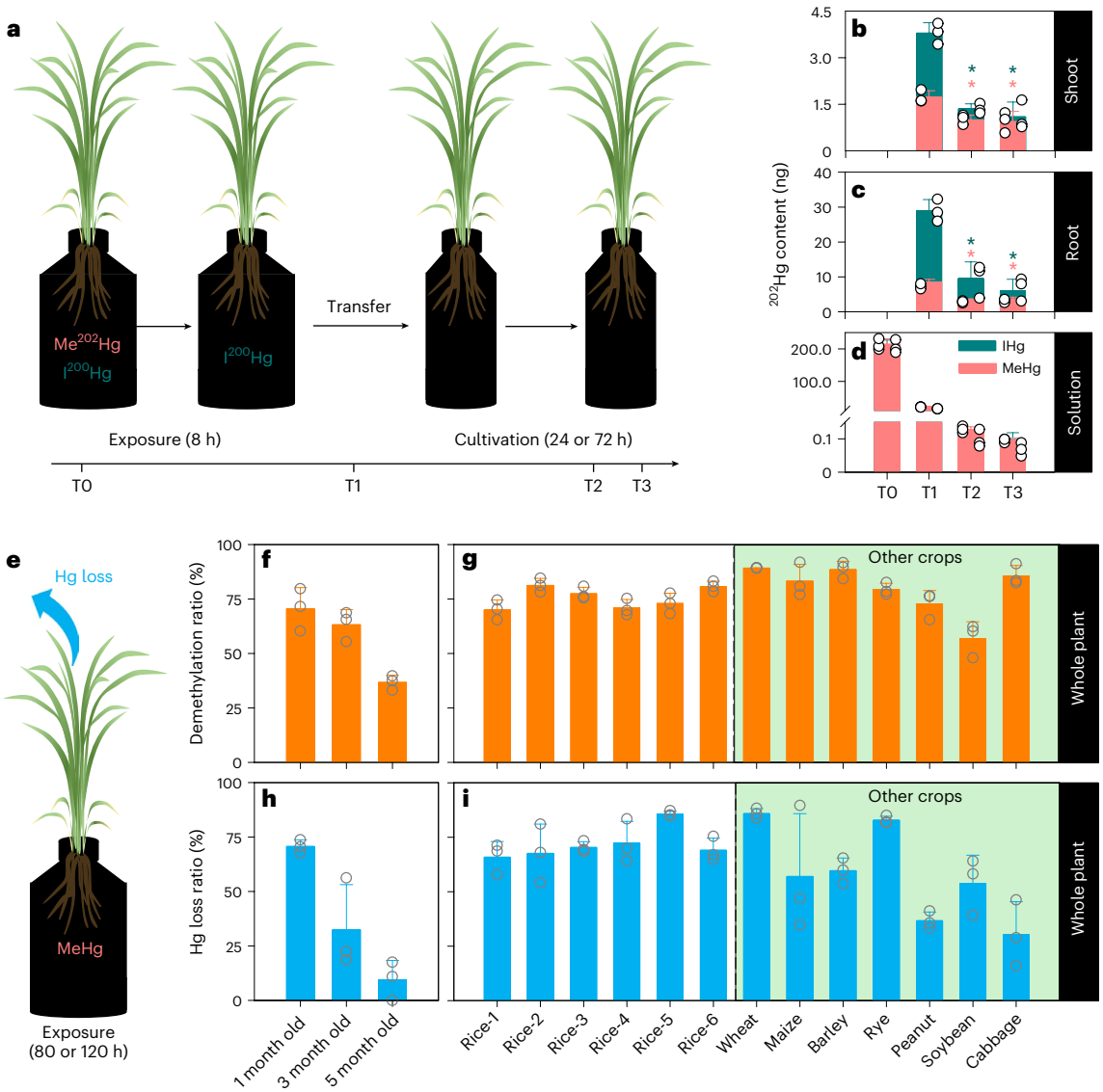

Fig. 1 | Evidence of MeHg demethylation in vivo and Hg release from crops. **a**, Experimental set-up. **b**–**d**, The mass of ^{202}Hg in tissues (**b**, shoot and **c**, root) and exposure/cultivation solutions (**d**) in the enriched isotope experiment. The number of circles on the left and right margins of each bar correspond to three replicates of MeHg and THg, respectively. **e**, Experimental design. **f**,**g**, MeHg demethylation ratios and **h**,**i**, Hg loss ratios in rice growth stage experiment (**f**,**h**) and crop experiment (**g**,**i**); each replicate is depicted as a circle on the bar. T0 and T1 refer to the time when exposure started (with $Me^{202}Hg$ and $I^{200}Hg$ spiked into solutions) and ended (only a significant proportion of $I^{200}Hg$ remained in the solution; Supplementary Text 3); T2 and T3 refer to times when plants were further cultivated in Hg-free solution for 24 h (T2) and 72 h (T3). The demethylation ratio is the proportion of demethylated MeHg to total MeHg absorbed by plants; total adsorbed MeHg is calculated by subtracting MeHg contents that remained in the solution after exposure and in root washing solutions from the total MeHg content in the solution before exposure; demethylated MeHg is calculated by subtracting MeHg contents detected in plants and in shoot washing solutions from total absorbed MeHg. Hg loss ratio is the ratio of the content of lost THg to total THg absorbed by plants from roots; total absorbed THg is calculated by subtracting the THg content that remained in solution after exposure and in root washing solutions from the total THg content in solution before exposure; lost Hg is calculated by subtracting THg contents detected in plants and in shoot washing solutions from total absorbed THg. The contents of THg and MeHg are calculated as a total mass (ng) to exclude the effect of variability in biomass. Asterisks (*) indicate significant ($P < 0.05$, one-way analysis of variance (ANOVA)) differences between two time points. All values are presented as mean ± s.d., $n = 3$ replicates. Some error bars may be too small to be visible in graphs. Details of each replicate can be found in source data.

identified as a major dietary source of MeHg[21] and is responsible for up to 96% of the MeHg exposure in inland China[22]. More importantly, rice is the most common food ingredient in ready-to-eat formulas for infants, contributing approximately half of their MeHg exposure and putting them at greater risks compared with adults[23]. Deciphering the pathway of plant-mediated demethylation is therefore critical to understanding how MeHg makes its way from soils to crops and then to humans. However, it is challenging to distinguish demethylation driven by plants themselves, rhizospheric/endophytic microorganisms and/or light, all of which are entangled in the complex soil–plant system[17,19]. Tackling this challenge requires tracing Hg transformations within plants and ruling out the contributions of both microbial demethylation and photolysis[19], by using multidisciplinary tools and providing multiple lines of evidence.

Results and discussion

Demethylation occurs within crops

In this Article, we explore MeHg demethylation within rice plants using an enriched Hg isotope tracer approach. During the cultivation of rice seedlings in a non-Hg-spiked nutrient solution after exposure

https://doi.org/10.1038/s43016-023-00910-x

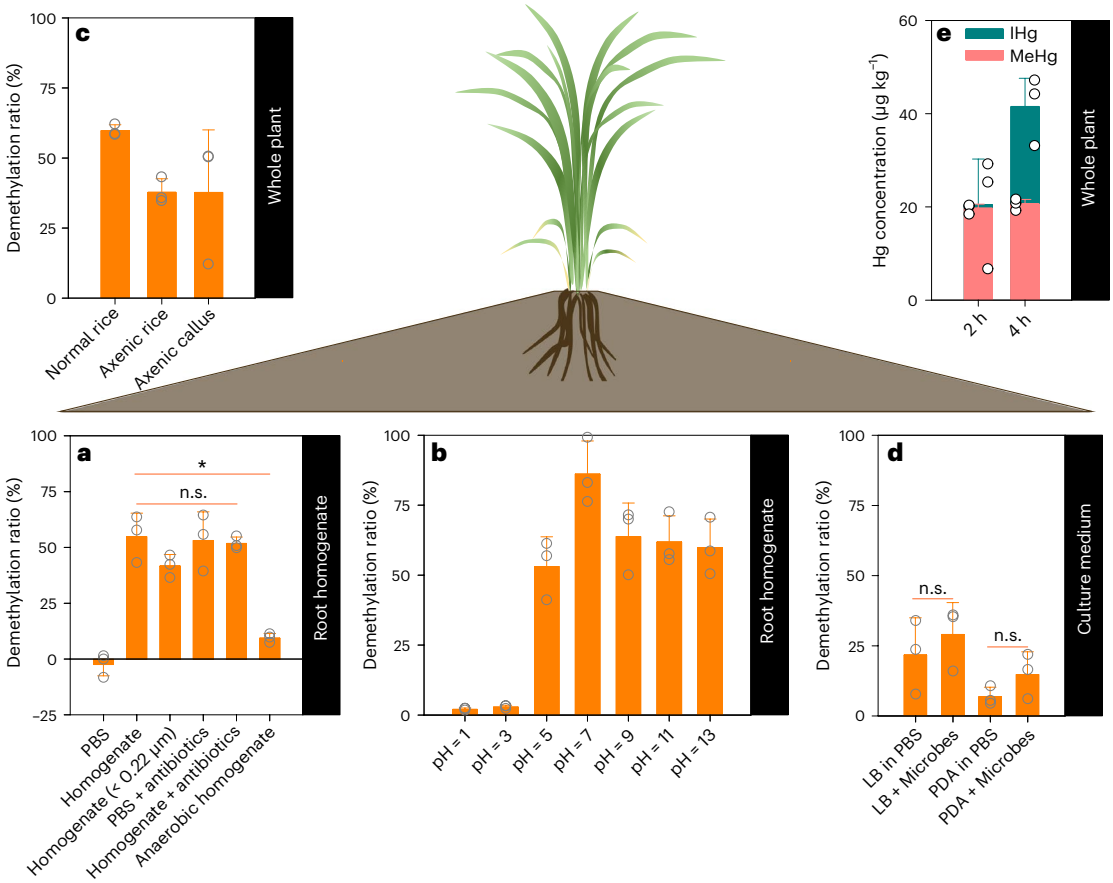

Fig. 2 | Lines of evidence showing in vivo MeHg demethylation irrespective of microorganisms. a–**e**, MeHg demethylation ratios in **a**, homogenates with microbes excluded or inhibited, **b**, homogenates under different pH, **c**, normal and axenically cultured rice plants/callus (2 weeks old), **d**, media with/without isolated microorganisms and **e**, Hg concentrations in whole rice plant after being exposed to dissolved MeHg for 2 h and 4 h. PBS refers to phosphate buffer (Na/K, 20 mM, pH = 7.0), and LB and PDA represent the media for bacteria and fungi, respectively. In **a**, PBS and PBS + antibiotics were set as control groups; the treatment of anaerobic homogenate means roots were homogenized and incubated both under anaerobic conditions. In **c**, normal rice refers to rice seedlings cultivated in an environmental chamber, and axenic rice and callus indicate those cultivated in a sterilized environment. In **e**, the presented Hg concentrations are the differences between the Hg concentrations in plants exposed to dissolved MeHg and those in plants exposed to non-spiked $CaCl_2$ solution. Both normal rice and axenically cultivated rice in **c** were 2 weeks old; n.s. indicates no significant differences ($P > 0.05$, one-way ANOVA) between two treatments. Data are presented as mean ± s.d., $n = 3$ replicates. Each replicate is depicted as a circle on the bar, and details of each replicate can be found in Source Data.

to dissolved $Me^{202}Hg$ (Fig. 1a), we observe mass decreases in either $Me^{202}Hg$ or ambient MeHg (naturally occurring MeHg, further discussed in Supplementary Text 1) in rice tissues (Fig. 1b,c and Extended Data Fig. 1a–c), reflecting that MeHg demethylation occurs within plants. Meanwhile, the accumulation of inorganic ^{202}Hg ($I^{202}Hg$, calculated as the difference between total ^{202}Hg and $Me^{202}Hg$; Fig. 1b,c) is also observed during cultivation, providing evidence that decreases in $Me^{202}Hg$ are due to the transformation of $Me^{202}Hg$ to $I^{202}Hg$. The $I^{202}Hg$ observed in rice plants is not derived from the uptake of $I^{202}Hg$ by roots as it is undetectable in the exposure medium or root washing solutions (Fig. 1d and Extended Data Fig. 2). Conversely, Hg methylation within plants is not supported by our data as no $Me^{200}Hg$ is detected in rice tissues after exposure to dissolved $I^{200}Hg$ (Extended Data Fig. 1d,e and Supplementary Text 2).

The demethylation of MeHg occurs within rice plants at all growth stages (showing a demethylation ratio of 37–71%, particularly at the early stages; Fig. 1f), and the demethylation ratios are consistently high in five other varieties of rice and in seven other major crop species (61–90%; Fig. 1g). Moreover, our data also support that MeHg demethylation occurs predominantly in roots, as a higher proportion of inorganic Hg (IHg, calculated as the difference between THg and MeHg) is found in roots than that in shoots following MeHg exposure (30–95% in roots versus 10–63% in shoots; Supplementary Text 4). In addition, demethylation occurs regardless of MeHg exposure concentrations (0–100 μg l^{-1}) or the presence of soil pore water (Extended Data Fig. 3 and Supplementary Text 5), supporting the representativeness of these experimental findings to natural environments.

In addition to the transformation of MeHg into IHg within plants, we report the subsequent reduction and release of Hg into the air following demethylation. The mass of total isotopic Hg in rice tissues (THg, for either ^{202}Hg or ^{200}Hg) decreases significantly during the course of the enriched isotope experiment (Fig. 1b,c and Extended Data Fig. 1d,e). Similarly, Hg loss from plants during MeHg exposure is also observed at different growth stages of rice, in different rice varieties and other crop plants, with loss ratios of 0–71%, 66–86% and 30–86%, respectively (Fig. 1h,i). By carrying out the Hg-release experiment in a closed system (Extended Data Fig. 4), we detect only Hg^0 and no other Hg species in the surrounding air after exposing rice plants to dissolved MeHg, with the amount of released Hg^0 being 1.8 times higher than that from plants exposed to the non-spiked solution. The released Hg^0 does not originate from the exposure solution nor from roots, considering that THg and MeHg concentrations are comparable in exposure medium and tissue washing solutions (Extended Data Figs. 2 and 5), and thus the content of dissolved Hg^0 is extremely low. Instead,

https://doi.org/10.1038/s43016-023-00910-x

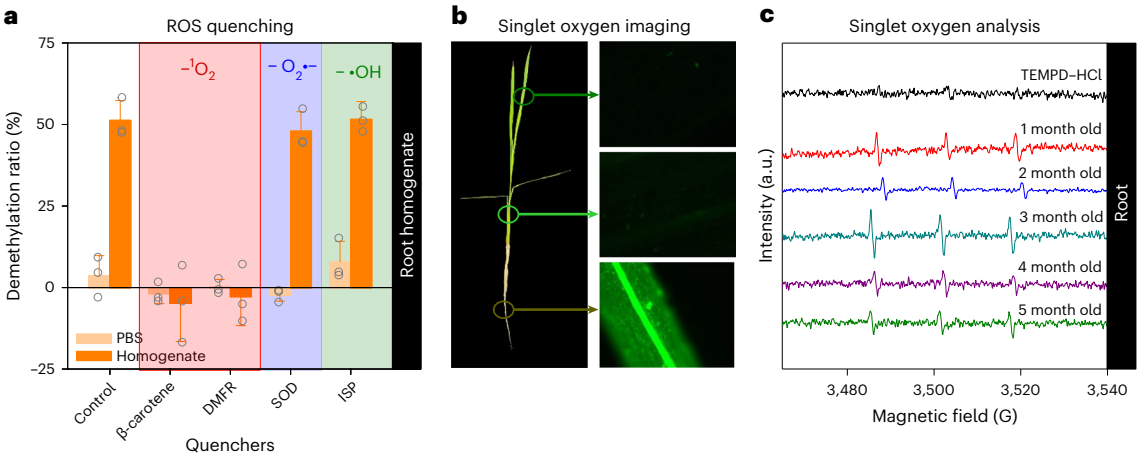

Fig. 3 | Lines of evidence showing the dominant role of singlet oxygen in MeHg demethylation in rice plants. a, The response of MeHg demethylation in root homogenates to radical quencher additions. **b**, The appearance of singlet oxygen in different tissues using SOSG. **c**, The signal of singlet oxygen from rice roots using EPR. In **a**, β-carotene (10 mM) and dimethylfuran (DMFR, 50 mM) are quenchers of singlet oxygen; superoxide dismutase (SOD, 0.5 mg l^{-1}) is a quencher of the superoxide anion ($O_2^{\bullet-}$); isopropyl alcohol (ISP, 50 mM) is a quencher of the hydroxyl radical (•OH). In this experiment, demethylation ratio is defined as the proportion of demethylated MeHg to total spiked MeHg, where the demethylated MeHg (μg l^{-1}) is calculated by subtracting the remaining MeHg (μg l^{-1}) from total spiked MeHg (μg l^{-1}). Phosphate buffer (PBS, Na/K, 20 mM, pH = 7.0) was set as a control, and the root homogenate was obtained by grinding rice roots in PBS (pH = 7.0) at a ratio of 1 g fresh tissue per 10 ml PBS. Data are presented as the mean ± s.d., $n = 3$ replicates. Each replicate is depicted as a circle on the bar, and details of each replicate can be found in Source Data. In **c**, the black line indicates the EPR signal from 500 mM TEMPD–HCl (dissolved in 20 mM PBS buffer/D_2O, pH = 7.0), while coloured lines indicate the EPR signal from fresh roots at different growth stages (rice plants cultivated in 2 ml of 500 mM TEMPD-HCl dissolved in 20 mM PBS/D_2O). a.u., arbitrary unit.

the released gaseous Hg^0 is derived from the in vivo transformation of the absorbed MeHg. By spiking $Me^{199}Hg$ into the exposure solution, we find a notable amount of $^{199}Hg^0$ (3.6 ng; details in Supplementary Text 6) is captured from the ambient air. This provides direct evidence that rice plants could release Hg^0 to the ambient air after MeHg absorption and its in vivo transformation.

The exchange of Hg between soil and air is a key process in global Hg cycling, whereas how plants channel Hg flux to the air is unclear[24]. Our results decipher this process by revealing that a sequence of MeHg uptake–MeHg demethylation–IHg reduction by plants is an efficient pathway of soil–air Hg exchange, during which Hg is in vivo transformed from the most bioavailable and neurotoxic species (that is, MeHg) into less bioavailable and less toxic species (that is, IHg and Hg^0)[25]. We further estimate that Hg release from rice plants via this process is ~30-fold (ranging 2-fold to 2,907-fold) greater than that via IHg uptake–IHg reduction (calculated using the Hg release capacities obtained from the enriched isotope experiment and the documented MeHg-to-IHg ratios in pore water; details in Supplementary Information, Methods Section 1). The relatively large uncertainty range is mainly attributed to variations in the reported MeHg-to-IHg ratios (Supplementary Table 1). However, further studies are warranted to assess the amount of Hg release via the process (that is, MeHg uptake–MeHg demethylation–IHg reduction by plants), especially in the field, as well as the relative importance of this pathway and the direct Hg emission from soils, a well-recognized pathway of soil–air Hg flux[26–28].

Singlet oxygen induces the demethylation

To elucidate the pathway of MeHg demethylation within plants, we examine the potential involvement of microbial degradation and photolysis, the two most commonly recognized demethylation pathways[10–12]. We demonstrate that MeHg demethylation occurs irrespective of the presence of microorganisms. This is evidenced by the substantial demethylation in microbe-excluded supernatant of root homogenate (40%, <0.22 μm), in microbe-inhibited root homogenates (54% under antibiotics addition and 64–66% under alkaline conditions where most microorganisms cannot survive) and in axenically cultured rice plants (38%) and rice callus (38%) (Fig. 2a–c). These moderate differences in demethylation ratios between normal and axenic rice plants/callus are not attributed to microorganisms but to the differences in cultivation and exposure conditions (Supplementary Text 7). In addition, the minor role of microorganisms in demethylation is further supported by the incapability of demethylation by root-isolated (Fig. 2d) or rhizospheric microorganisms (Extended Data Figs. 2 and 5), higher demethylation under aerobic conditions than anaerobic ones (Fig. 2a and Supplementary Text 7) and the slower rate of demethylation documented for microorganisms (for example, half-life > 1 day in sediments)[14] compared to rice plants (half-life ~2 h; Fig. 2e). Meanwhile, MeHg demethylation within plants is light independent. This is due to the minor effect of light on MeHg demethylation both in living plants and in root homogenates (Extended Data Fig. 6), and most MeHg is demethylated in roots where light is absent (Fig. 1b,c and Supplementary Text 4).

Our analyses of reactive oxygen species (ROS) show that in vivo generated singlet oxygen is responsible for the observed demethylation within rice plants, being the mechanism of this light- and microbe-independent demethylation pathway. It has been reported that ROS such as singlet oxygen, hydroxyl radical and superoxide anion could induce the photolysis of MeHg in surface water[29,30]. However, ROS-mediated MeHg demethylation within organisms has been largely ignored, particularly for plants, although those ROS are commonly found in plant cell organelles including mitochondria, chloroplast and nucleus and irrespective of light[31,32]. Here we provide multiple lines of evidence that support the light- and microbe-independent demethylation of MeHg in plants driven by singlet oxygen. First, the additions of selective quenchers to the root homogenate inhibit MeHg demethylation by >70% only in the singlet oxygen-quenched treatments during the whole growth period of rice plants (Fig. 3a and Extended Data Fig. 7a). Second, we measure singlet oxygen in living plants using singlet oxygen sensor green (SOSG; Fig. 3b and Extended Data Fig. 7b) and in fresh root tissue (Fig. 3) and supernatant of root homogenate (<0.22 μm; Extended Data Fig. 8a) using electron paramagnetic resonance (EPR). At all growth stages, the signal of singlet oxygen is observed in rice plants, especially in roots (Fig. 3b and Extended Data

https://doi.org/10.1038/s43016-023-00910-x

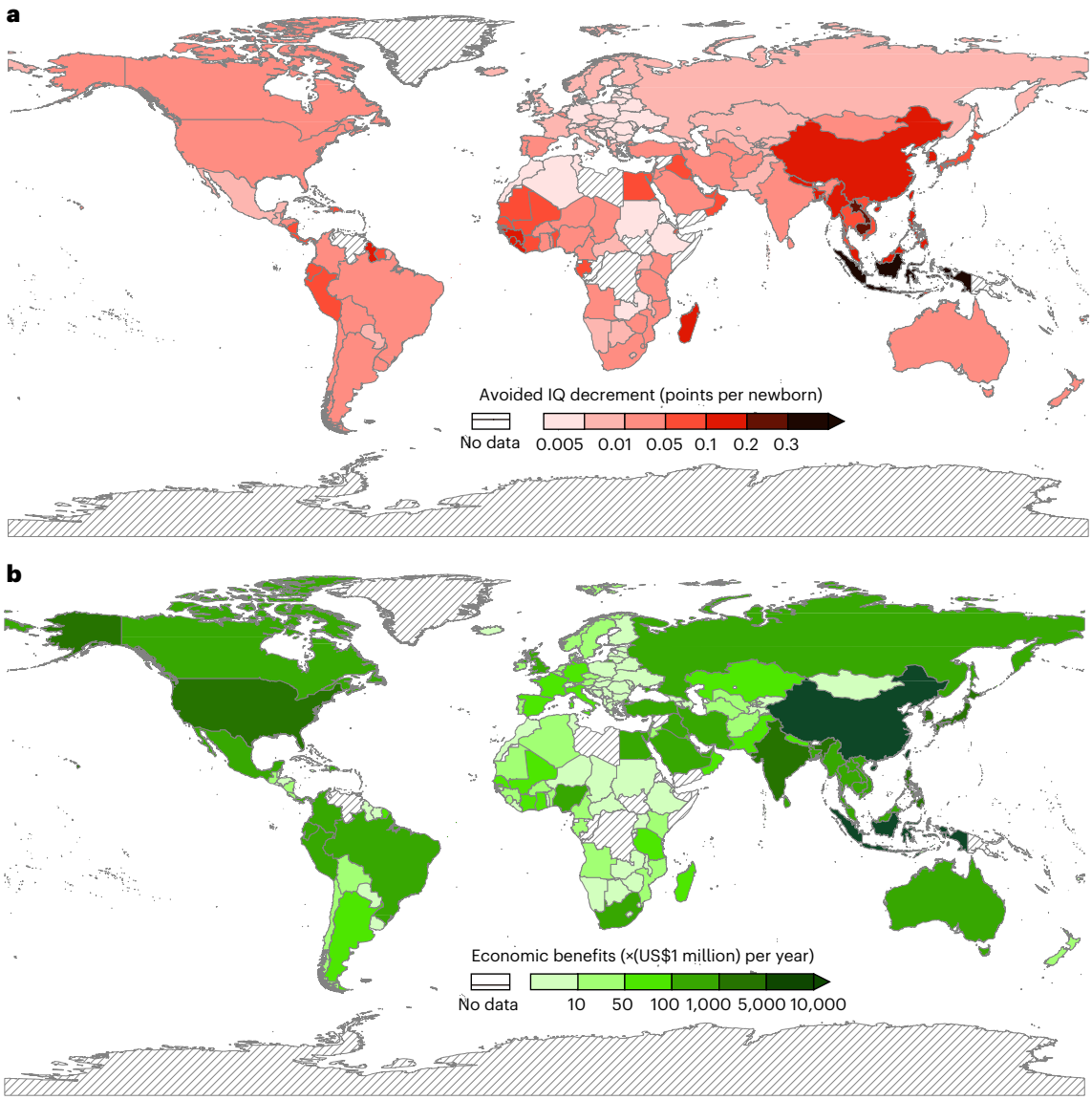

Fig. 4 | Health and economic benefits induced by MeHg demethylation in rice plants. a,**b**, Prevented IQ decrement (**a**) and the associated economic benefit (**b**) resulting from MeHg demethylation by rice plants. Only the data in scenario B are depicted here. More information can be found in Supplementary Tables 2 and 3 and Source Data (including all the related parameters for the calculations of IQ decrement and economic benefit). The global map is provided by Natural Earth (https://www.naturalearthdata.com/downloads/10m-cultural-vectors/, accessed on 18 October 2022).

Fig. 7b). It should be noted that the singlet oxygen detected in plants is not induced by homogenization or light irradiation (Extended Data Fig. 8 and Supplementary Text 8). Third, demethylation under singlet oxygen attack is further supported by results of density functional theory (DFT) calculations (Extended Data Fig. 9 and Supplementary Text 9) and the demethylation ratios quantified in a singlet oxygen-generating system (Extended Data Fig. 10). We thus propose that the complexation of MeHg with thiols, which are abundant in plants, could lower the activation barrier to break the Hg–C bond of MeHg, facilitating the electrophilic attack of the Hg–C bond by singlet oxygen (Supplementary Text 10). Considering that singlet oxygen commonly exists across microorganisms, plants and animals[33,34], more work is necessary to explore the importance of this hidden demethylation pathway in other taxa and in natural fields.

This in vivo demethylation mechanism differs fundamentally from previously reported ROS-mediated MeHg photolysis in surface water[29] and at the soil–water interface[35], considering that plant demethylation is light independent. Although ROS or non-oxygen-centred radical-induced MeHg demethylation in animals has been hypothesized in a few earlier studies[36–38], the ROS or radicals were generated by adding exogenous oxides or activators in vitro, while the in vivo generated ROS were not determined, and their roles in MeHg demethylation were unknown in those studies. In addition, the role of light or microorganisms in the observed MeHg demethylation of those previous studies was not excluded. Photolysis and microbial demethylation are commonly recognized as the dominant pathways that degrade MeHg in the ambient environment. The discovery of this light- and microbe-independent pathway expands beyond the boundaries of knowledge on MeHg degradation in nature, extending MeHg demethylation research from the ambient environment to flora and elucidating Hg transformation upon the initiation of bioaccumulation at the bottom of food webs.

Demethylation in rice mitigates exposure

We use a health risk model to assess the protective effects of MeHg demethylation within rice on human health. The cognitive deficit (ΔIQ) is

chosen to show the health endpoints based on epidemiological studies that have shown a linear dose–response relationship between maternal intake of MeHg and fetal IQ decrements[39–41]. By developing a MeHg accumulation model and applying Monte Carlo simulation, we estimate the IQ decrements prevented by MeHg demethylation within rice in 159 countries/regions. Results show that MeHg demethylation within rice plants greatly reduces the concentrations of neurotoxic MeHg in rice grains, moderating IQ losses and providing economic benefits (Source Data). The results of the modelling analysis show that, in the absence of MeHg demethylation within rice plants, MeHg levels in rice grains would increase by a factor of 2.4 (scenario A, simulating the minimum MeHg demethylation within rice plants; Supplementary Information Methods Section 2) or 4.7 (scenario B, simulating the maximum MeHg demethylation within rice plants), leading to increased human exposure to MeHg. For instance, in Indonesia, ranking third in rice production and fourth in population in the world, the observed rice MeHg concentration averages at 4.6 μg kg^{-1} (ref. 42), while it would increase to 10.6 μg kg^{-1} (scenario A) or 21.1 μg kg^{-1} (scenario B) without in vivo demethylation. Under the assumption that the average body weight of Indonesians is 60 kg, the estimated daily intake of MeHg from rice consumption would be 0.07 μg (scenario A) or 0.13 μg (scenario B) MeHg per kg body weight per day, comparable to or higher than the maximum acceptable oral dose suggested by the US Environmental Protection Agency (0.1 μg MeHg per kg body weight per day). The reductions in rice MeHg levels resulting from demethylation within plants avoid IQ decrements by 0.01–0.19 (scenario A, with a P90 of 0.03–0.44; Supplementary Table 2) or 0.03–0.51 points per fetus (scenario B, with a P90 of 0.07–1.22; Supplementary Table 2) in regions with high rice consumption (>100 g per capita per day; Fig. 4a). Taking the mainland of China for example, the prevented IQ decrements are 0.04–0.11 points per newborn, which are comparable to the total IQ decrements caused by dietary MeHg exposure in China (0.14 point)[7].

These modelled results clearly show the importance of MeHg demethylation within rice plants for protecting human health. Previous studies have shown that IQ deficits have direct and indirect effects on lifetime earnings[43,44]. Combining the coefficient of IQ to lifetime earnings, the prevented IQ decrement and the annual number of new births in an area (Supplementary Information, Methods Section 2), we estimate the annual economic benefits generated as a result of MeHg demethylation within rice plants to be US$30.7–84.2 billion globally. Among all the studied countries, China, Indonesia, India, the US and Japan are the top five countries benefiting the most from MeHg demethylation in rice plants (Fig. 4b), with average annual benefits of US$15.8, US$6.5, US$1.3, US$1.2 and US$0.4 billion (scenario A, with a P90 of 36.3 15.3, 2.2, 3.5 and 0.9, respectively; Supplementary Table 3) or US$43.8, US$17.2, US$3.5, US$3.3 and US$1.2 billion (scenario B, with a P90 of 101.0, 40.8, 6.1, 9.5 and 2.6, respectively; Supplementary Table 3). Indeed, these benefits may even surpass those from controlling Hg emissions, the primary ongoing global strategy for mitigating MeHg risks. For instance, in China, the predicted economic benefits provided by MeHg demethylation in rice are US$15.8 billion (scenario A) or US$43.8 billion (scenario B), which are appreciably higher than the US$8.4–21.6 billion associated with the Hg emission control processes used in coal-fired power plants each year[45].

Our study reveals that plants act as a 'channel' of Hg flux from the pedosphere to the atmosphere through efficient MeHg uptake by roots from the soil, rapid transformation in vivo irrespective of light/microbes and then the release of Hg^0 to the air. As a result, Hg is effectively removed from plants and re-directed to the air, and the observed MeHg bioaccumulation thus represents only a small proportion of MeHg absorbed by plants. Our results show that plants provide a highly beneficial ecosystem service by degrading MeHg in vivo thereby mitigating Hg flux to food chains. These findings call for rethinking the roles of plants in global Hg cycling. Further studies should quantify Hg^0 release following in vivo demethylation in other systems such as forest and ocean, which would improve the mapping of global Hg cycling. We also call immediate attention from scientific communities to the future changes in the effectiveness of this natural barrier against MeHg accumulation in crop plants, for example, under climate change which would impact plant physiology and ROS generation[46] and thus the global food security.

Methods

Experimental designs

A series of experiments were designed to confirm the occurrence of MeHg demethylation in crops, quantify the demethylation capacity and reveal the potential mechanism, as presented below and summarized in Supplementary Table 4.

Enriched isotope experiment. MeHg demethylation within rice plants was examined by applying the enriched isotope tracing technique. Briefly, rice seedlings (Wufeng, referred to as Rice-1) were cultivated hydroponically for 1 month in a climate-controlled plant growth chamber (25 °C, 14 h:10 h light:dark, the same for all exposures). A total of 45 seedlings with similar heights were selected and exposed to 0.01 M $CaCl_2$ solution spiked with ~0.4 μg l^{-1} $Me^{202}Hg$ (as $CH_3{}^{202}HgCl$, 97.7%) and ~0.15 μg l^{-1} $I^{200}Hg$ (as $^{200}Hg(NO_3)_2$, 79.7%). These Hg contents were chosen according to the reported values in paddy pore water[47] and MeHg/THg ratios in the pore water of wetlands and sediments (Supplementary Table 1), considering that data on MeHg in paddy pore water and MeHg/THg ratios are limited. The time when exposure started was defined as T0. $CaCl_2$ solution instead of soil pore water was used to exclude the effects of soil dissolved organic matter on MeHg uptake by plants and plant growth (Supplementary Text 5). After 8 h of exposure (T1), 15 seedlings were selected randomly and subjected to isotopic Hg analyses. The remaining 30 seedlings were transferred to 6 bottles, and each bottle contained 5 seedlings and 100 ml of nutrient solution (Hg free). These six bottles were placed in the growth chamber for further cultivation for 24 h (T2) or 72 h (T3) to investigate the dynamic of MeHg demethylation. After cultivation, all seedlings were collected and separated into shoots and roots. Then, the tissues were washed sequentially with 8 mM cysteine solution and deionized water, oven dried to constant weight (at 40 °C) and ground for Hg analyses. The efficiency of the washing procedure to remove surface-adsorbed MeHg has been tested in a previous experiment[48]. All the liquids, including the media before and after uptake, cysteine and deionized washing solutions (referred to as washing solutions) and nutrient solution were collected with weights recorded and then acidified using HCl before Hg isotope analyses.

Rice growth stage experiment. To explore the demethylation capacity of rice plants at different growth stages, rice plants (Rice-1) were cultivated hydroponically in a growth chamber for 1, 3 and 5 months and then exposed to a 0.8 μg l^{-1} MeHg solution (containing 0.01 M $CaCl_2$) at room temperature. After 80 h exposure, the plants were collected, washed (shoots and roots separated) and dried as described above. Solutions were also collected with weights recorded. All the plant tissues and solutions were subjected to MeHg and THg analyses.

Crop experiment. Six varieties of rice plants and seven common crop plants were selected to quantify MeHg demethylation in vivo. These rice varieties (that is, Wufeng, Liangyou900, Xiangliangyou900, Akitakomati, Yueguang and Jingliangyouhuazhan, referred to as Rice-1, Rice-2, Rice-3, Rice-4, Rice-5 and Rice-6, respectively) are commonly planted in China, and these crop plants, that is, rice, wheat, maize, barley, rye, peanut, soybean and cabbage are common crops according to the planting area worldwide (based on the Food and Agriculture Organization database). After being cultivated hydroponically for 1 month, each variety was exposed to 80–500 ml (depending on the biomass of each species) of 100 μg l^{-1} MeHg solution (containing 0.01 M

$CaCl_2$) or 0.01 M $CaCl_2$ for 5 days. A 5 day exposure period was used, considering that MeHg demethylation in rice plants occurs within hours to days according to the results of our preliminary experiments. A relatively high concentration of MeHg, that is, 100 μg l^{-1}, instead of an environmentally relevant concentration, was applied to minimize the interference of background Hg, also considering that MeHg demethylation occurs regardless of the exposure concentrations (Extended Data Fig. 3 and Supplementary Text 5). After exposure, all seedlings were collected, washed (with shoots and roots separated) and dried as described above before THg and MeHg analyses. All liquids, including media before and after exposure, cysteine and deionized washing solutions, were collected with weights recorded and then acidified with HCl to measure Hg levels.

Demethylation-impacting factor experiments. To explore possible factors that may impact MeHg demethylation, we quantified demethylation ratios under different conditions both in vivo and in vitro. Specifically, the effects of light, microorganisms and exposure concentration/matrix/duration on MeHg demethylation in vivo, as well as the effects of light, pH and microorganisms on MeHg demethylation in vitro, were explored using Rice-1. Details of the experimental design are summarized in Supplementary Tables 5 and 6.

For in vivo tests, rice plants were cultivated hydroponically and then subjected to MeHg exposure, as shown in Supplementary Table 5. After exposure, rice plants were collected, washed and analysed for THg and MeHg concentrations. All the solutions were collected, weighed and acidified before Hg analyses. The axenically cultured rice/callus (2 weeks, Rice-1, cultivated in Sihai Yang's lab, Nanjing University) were also used to quantify demethylation after being exposed to dissolved MeHg.

For in vitro tests, the roots of 1-month-old rice seedlings were homogenized in phosphate buffer in ice bath. Roots instead of the whole plant/shoots were used as roots are more capable of MeHg demethylation. These homogenates were then spiked with MeHg to a level of 100 μg l^{-1} and incubated at room temperature for 5 days. To evaluate the roles of rhizospheric and/or endophytic bacteria in MeHg demethylation (such as endophytes)[49], antibiotics (1% penicillin–streptomycin solution, *v*/*v*; GE Healthcare Life Sciences) were added to the homogenate. The demethylation in the supernatant fraction of homogenate (filtered by 0.22 μm membrane to exclude microorganisms, ASTM F838-05) was also explored. After incubation, all homogenates were analysed for MeHg concentrations. The microbial community in homogenates (with or without antibiotics) was analysed before and after incubation (16S ribosomal RNA, Sangon Biotech).

In addition, the role of culturable microorganisms isolated from roots in MeHg demethylation was also investigated. Briefly, fresh roots of Rice 1 (1 month old) were surface sterilized[50], washed with sterilized deionized water seven times and homogenized, and then the homogenates were inoculated into Luria–Bertani (LB, for the cultivation of bacteria) or potato dextrose agar (PDA, culture medium for fungi) solid medium. Three replicates were set for either bacteria or fungi. After inoculation, the plates with endophytic bacteria were cultivated at 37 °C, while the endophytic fungi were cultivated at 28 °C. After 10 days of cultivation, 2.5 ml of sterilized PBS solution (pH = 7.2) was added to each plate to wash the colonies. Then the PBS containing endophytes was transferred to sterilized centrifuge tubes. After mixing thoroughly, the optical densities (OD600, Infinite 200 pro, TECAN) of the PBS solutions were measured to determine the growth of endophytes. Next, the OD600s of all the PBS containing endophytic bacteria or fungi were adjusted to 0.5 using PBS. A volume of 500 μl bacterial/fungal solution was then mixed with 500 μl sterilized LB/PDA, spiked with MeHg (10 μg l^{-1}) and then cultivated at 25 °C in the dark to quantify possible MeHg demethylation. After 5 days of cultivation, samples were collected to analyse the remaining MeHg. Meanwhile, the demethylation capacity of LB or PDA medium was also quantified. Specifically, 500 μl of cultivation medium was mixed with 500 μl PBS solution (20 mM). Then MeHg was spiked into each replicate to a final concentration of 10 μg l^{-1}, and the mixtures were incubated as described above. After 5 days of incubation, samples were collected to analyse the remaining MeHg.

Hg release experiment. To identify the Hg species after MeHg demethylation, rice plants (Rice-1) were exposed to dissolved MeHg in a closed system (Extended Data Fig. 4). Specifically, two treatments, that is, control (0.01 M $CaCl_2$ solution) and exposure treatment (~0.4 μg l^{-1} MeHg in 0.01 M $CaCl_2$ solution) were designed. Each treatment contained three replicates, and each replicate contained five rice seedlings. The bottle with the exposure medium was sealed with Parafilm to prevent the contact of solution with the chamber. The chamber and the bottle holding the exposure medium were connected and sealed with Parafilm and tape. Compressed air, with residual Hg removed using a gold trap, was introduced into the chamber at a flow of ~30–50 ml min^{-1}. The air exiting the chamber was introduced to a gold trap (filled with gold-coated quartz) for Hg^0 collection or a Tenax-TA trap column (filled with Tenax-TA, an adsorbent for organic Hg) to collect Hg^0 and organic Hg species. After 80 h of exposure, the chamber was separated from the bottle holding the uptake medium and capped immediately, ventilated for 30 min and washed with 5% BrCl solution. All the seedlings were washed (with shoots and roots separated) and dried as described above. All the solutions were acidified with HCl for THg and MeHg analyses. The recovery rate of Hg was monitored and found to be satisfactory (107%; details in Supplementary Table 7) for this closed system. To identify the source of the trapped Hg, this experiment was repeated (exposure treatment only) with the application of enriched $Me^{199}Hg$. The content of captured Hg^0 was analysed using inductively coupled plasma mass spectrometry (ICPMS).

Quencher addition experiments. To explore the potential roles of ROS in MeHg demethylation in plants, we quantified MeHg demethylation in response to quencher addition in root homogenates (obtained in ice bath) of 1-, 2- and 4-month-old rice plants. Specifically, β-carotene (10 mM, >96%, Aladdin), tetrahydrofuran (50 mM, 99.5%, J&K) and dimethylfuran (50 mM, >99%, Damas-beta) were used to quench singlet oxygen; superoxide dismutase (0.5 mg l^{-1}, derived from swine blood, Shanghai Yuanye Biotechnology) was used to quench superoxide anion, and isopropyl alcohol (50 mM, >99.9%, Aladdin) was used to quench hydroxyl radical[51]. Homogenates and PBS were added with quenchers and spiked with MeHg (100 μg l^{-1}). After being incubated for 5 days at 30 °C in the dark, homogenates were analysed for MeHg contents.

Singlet oxygen-generating chemical system. To provide further evidence that singlet oxygen induces MeHg demethylation in the presence of thiols, we quantified demethylation in a singlet oxygen-generating chemical system, that is, molybdate and H_2O_2. Specifically, 100 μl of molybdate and 50 μl of reduced glutathione (GSH) were added to PBS (900 μl) to a final concentration of 25 mM and 20 μM, respectively (refers to singlet oxygen + GSH). Then 10 μl of MeHg standard solution (1 mg l^{-1}, Brooks Rand) was added and equilibrated for 1 h. PBS and treatment without GSH (singlet oxygen treatment) were set as controls to quantify the demethylation capacities of PBS buffer and singlet oxygen. The demethylation capacities of GSH, molybdate and H_2O_2 alone were quantified and found to be negligible. After the equilibration, 10 μl of H_2O_2 (7.5%, *w*/*v*) was added to treatments of singlet oxygen + GSH and singlet oxygen. The addition of H_2O_2 was repeated 5 times with a time interval of 40 min. Such an operation was designed to maintain a continuous generation of singlet oxygen. Thirty to forty minutes after the last addition, MeHg in each treatment, as well as MeHg in solutions before H_2O_2 addition, were detected for the calculation of the demethylation ratios.

Parameter analyses

Hg analysis. For isotopic THg, water samples were subjected to digestion with BrCl, while plant samples were digested by a mixture of HNO_3 and H_2SO_4 (7:3, *v*/*v*). ^{201}HgCl was added to all samples as an internal standard. After the reduction by $SnCl_2$, Hg was measured using ICPMS[52]. For isotopic MeHg analysis, both water and plant samples were distilled, ethylated and then measured using gas chromatography (GC)-ICPMS. Me^{201}Hg was added to each sample as the internal standard. Analysis of duplication, matrix spikes and standard reference materials (for THg, lobster muscle, TORF-3, 290 ± 2.2 μg kg^{-1}; for MeHg, estuarine sediment, BCR-CRM 580, 75 ± 4 μg kg^{-1}) were included in each analytical session. Isotope dilution calculations and further details could be found in Hintelmann and Ogrinc[53]. It should be noted that due to the relatively low enrichment of spiked I^{200}Hg, the enrichments of other Hg isotopes were subtracted according to the proportions of each isotope (obtained from the manufacturer) during the calculation. The recoveries of standard reference material were 90–96% (n = 3) for THg and 91–107% (n = 4) for MeHg. The recoveries of matrix spike for water digestion (THg) were 88–109%, and the relative standard deviations for duplicated distillation and analysis were <10%.

For ambient THg analysis, samples were analysed using an automated Hg analyser (Brooks Rand) after digestion with concentrated HNO_3 and H_2SO_4 (7:3, *v*/*v*). Analytical duplicates and standard reference material (citrus leaf, GBW10020, 150 ± 20 μg kg^{-1}) were applied to each batch of analysis, and the recoveries of the standard reference material were 105 ± 10% (n = 16) for THg. The recoveries of matrix spike were 95 ± 7% (n = 12). For MeHg, plant samples were digested with 2 ml of 25% (*w*/*w*) KOH–CH_3OH at 60 °C for 4 h, and then the concentrations were determined using an automated MeHg analyser (Brooks Rand), based on US Environmental Protection Agency Method 1630. Matrix spike and standard reference material (BCR-CRM 580) recoveries ranged from 88% to 105%. The effects of various ROS quenchers on MeHg analyses were checked by standard addition, and the recoveries ranged from 91% to 105% (Supplementary Table 8).

Hg species in traps from the Hg release experiment were analysed using manual Hg analysis systems. Specifically, for organic Hg analysis, the Tenax-TA trap columns were heated to 120 °C within 30 s. All adsorbed Hg was released and separated through a GC column (15% OV3, 680 mm; temperature, 30 °C; Ar flow, 50 ml min^{-1}), pyrolysed to elemental Hg and analysed by atomic fluorescence spectroscopy (Brooks Rand). Due to the high toxicity of dimethylmercury (DMHg), the instrument response to MeHg standard was used to quantify DMHg. The GC peak between elemental Hg and MeHg is identified as DMHg. For elemental Hg analysis, gold trap columns were heated to 500 °C within 15 s under a stream of Ar (50 ml min^{-1}). The Hg was then analysed by atomic fluorescence spectroscopy. For the analysis of $^{199}Hg^0$, trapped Hg was desorbed at 500 °C and introduced into a $KMnO_4$ solution with flowing Ar, and then the solution was neutralized with hydroxylamine hydrochloride before the analysis using ICPMS.

Singlet oxygen analysis. Singlet oxygen from rice roots was detected using EPR (E500, Bruker). 2,2,6,6-Tetramethyl-4-piperidone hydrochloride (TEMPD–HCl, 500 mM, Dojindo, Japan, prepared with 20 mM phosphate buffer/D_2O, pH = 7) was used as the spin trap[54]. D_2O, instead of H_2O, was used to prepare the phosphate buffer, considering that singlet oxygen has a longer lifetime in D_2O[55]. Roots of rice plants (1, 2, 3, 4 and 5 months old) were exposed to 2 ml of TEMPD-HCl for 1 h, after which the solution was subjected to the detection of singlet oxygen; meanwhile, the 20 mM phosphate buffer/D_2O was taken as the blank. EPR conditions were as follows: microwave frequency, 9.84 GHz; microwave power, 6.325 mW; field modulation frequency, 100 kHz; amplitude, 0.1 mT; sweep width, 200 G; sampling time, 40 s; and receiver gain, 42 dB.

In addition, singlet oxygen in shoots and roots was imaged using SOSG (Meilunbio) as the probe molecule[33]. Specifically, rice plants at ages of 1, 2 or 4 months were completely immersed in a 50 μM SOSG solution and cultivated for 30 min in the dark, then rinsed with deionized water three times and photographed with a fluorescence microscope (Zeiss Axio Imager.A). Singlet oxygen detection was conducted by recording the fluorescence emission spectra of SOSG (excitation/emission = 504/525 nm) with the excitation wavelength fixed at 488 nm.

Model estimation

This model was developed to evaluate the protective effects of rice-mediated demethylation on human health in non-Hg-contaminated areas. This evaluation is essential, considering that (1) rice consumption is a major source of dietary MeHg exposure for Asians due to the high consumption rate of rice, for example, accounting for up to 96% of MeHg exposure in China[22]; (2) even low-level dietary exposure to MeHg during pregnancy negatively affects a newborn's lifelong IQ[41]. It is also important to note that although photolysis and microbial demethylation may also contribute to reducing MeHg accumulation in rice, their potential contributions are excluded in model estimation. This is because the demethylation ratios used in the estimation are quantified under conditions with the interferences of both photolysis and microbial demethylation (Supplementary Text 7). Detailed descriptions of this section can be found in Supplementary Information, Methods.

DFT calculations

DFT calculations are carried out using the Gaussian 16 suite of programs[56], with meta-hybrid M06 functional[57] to investigate Hg–C bond cleavage in MeHg by singlet oxygen in the presence or absence of thiol (glutathione/GSH). The 6-311 + G(d,p) basis set (or 6-311 + G(d,p)//6-31 G(d) for system containing GSH) is used in geometry optimizations for all elements except Hg, for which ECP60MWB basis set is used to incorporate the Wood–Boring quasi-relativistic effective core potential (ECP)[58]. The spin contamination error of the system containing singlet oxygen is eliminated using the broken-symmetry solution by mixing the highest occupied molecular orbital and lowest unoccupied molecular orbital. Vibration analyses are performed for all complexes and transition structures to obtain zero-point energies and to confirm transition states. The solvent effect is computed in all calculations using the continuum solvation model density[59].

Reporting summary

Further information on research design is available in the Nature Portfolio Reporting Summary linked to this article.

Data availability

All the data supporting the findings are included in the main text, Supplementary Information and the Source Data. The databases used in this study are Food and Agriculture Organization (http://www.fao.org/faostat/#en/#dat), World Bank (http://data.worldbank.org/indicator/NY.GDP.PCAP.PP.CD and http://data.worldbank.org/indicator/NY.GDP.PCAP.KD.ZG), World Population Perspective 2019 (https://population.un.org/wpp/) and Natural Earth (https://www.naturalearthdata.com/downloads/10m-cultural-vectors/). Source data are provided with this paper.

References

1. UNEP. *Global Mercury Assessment 2018*. (UN Environment Programme, 2018).
2. Karagas, M. R. et al. Evidence on the human health effects of low-level methylmercury exposure. *Environ. Health Perspect.* **120**, 799–806 (2012).
3. Rice, G. E., Hammitt, J. K. & Evans, J. S. A probabilistic characterization of the health benefits of reducing methyl mercury intake in the United States. *Environ. Sci. Technol.* **44**, 5216–5224 (2010).

4. Bellanger, M. et al. Economic benefits of methylmercury exposure control in Europe: monetary value of neurotoxicity prevention. *Environ. Health* **12**, 1–10 (2013).
5. Grandjean, P., Pichery, C., Bellanger, M. & Budtz-Jørgensen, E. Calculation of mercury's effects on neurodevelopment. *Environ. Health Perspect.* **120**, 452 (2012).
6. Zhang, Y. et al. Global health effects of future atmospheric mercury emissions. *Nat. Commun.* **12**, 3035 (2021).
7. Chen, L. et al. Trans-provincial health impacts of atmospheric mercury emissions in China. *Nat. Commun.* **10**, 1484 (2019).
8. Seller, P., Kelly, C. A., Rudd, J. W. M. & Mac Hutchon, A. R. Photodegradation of methylmercury in lakes. *Nature* **380**, 694–697 (1996).
9. Klapstein, S. J., Ziegler, S. E., Risk, D. A. & O'Driscoll, N. J. Quantifying the effects of photoreactive dissolved organic matter on methylmercury photodemethylation rates in freshwaters. *Environ. Toxicol. Chem.* **36**, 1493–1502 (2017).
10. Kronberg, R. M., Schaefer, J. K., Björn, E. & Skyllberg, U. Mechanisms of methyl mercury net degradation in alder swamps: the role of methanogens and abiotic processes. *Environ. Sci. Technol. Lett.* **5**, 220–225 (2018).
11. Zhou, X. Q. et al. Microbial communities associated with methylmercury degradation in paddy soils. *Environ. Sci. Technol.* **54**, 7952–7960 (2020).
12. Wu, Q. et al. Methanogenesis is an important process in controlling MeHg concentration in rice paddy soils affected by mining activities. *Environ. Sci. Technol.* **54**, 13517–13526 (2020).
13. Barkay, T. & Gu, B. Demethylation—the other side of the mercury methylation coin: a critical review. *ACS Environ. Au* **2**, 77–97 (2022).
14. Feyte, S., Gobeil, C., Tessier, A. & Cossa, D. Mercury dynamics in lake sediments. *Geochim Cosmochim Acta* **82**, 92–112 (2012).
15. Hammerschmidt, C. R. & Fitzgerald, W. F. Photodecomposition of methylmercury in an arctic Alaskan lake. *Environ. Sci. Technol.* **40**, 1212–1216 (2006).
16. Lehnherr, I., St. Louis, V. L., Emmerton, C. A., Barker, J. D. & Kirk, J. L. Methylmercury cycling in high arctic wetland ponds: sources and sinks. *Environ. Sci. Technol.* **46**, 10514–10522 (2012).
17. Xu, X. et al. Demethylation of methylmercury in growing rice plants: an evidence of self-detoxification. *Environ. Pollut.* **210**, 113–120 (2016).
18. Li, Y. et al. The influence of iron plaque on the absorption, translocation and transformation of mercury in rice (*Oryza sativa* L.) seedlings exposed to different mercury species. *Plant Soil* **398**, 87–97 (2016).
19. Strickman, R. J. & Mitchell, C. P. J. Accumulation and translocation of methylmercury and inorganic mercury in *Oryza sativa*: an enriched isotope tracer study. *Sci. Total Environ.* **574**, 1415–1423 (2017).
20. Liu, J., Meng, B., Poulain, A. J., Meng, Q. & Feng, X. Stable isotope tracers identify sources and transformations of mercury in rice (*Oryza sativa* L.) growing in a mercury mining area. *Fundam. Res.* **1**, 259–268 (2021).
21. Liu, M. et al. Rice life cycle-based global mercury biotransport and human methylmercury exposure. *Nat. Commun.* **10**, 5164 (2019).
22. Gong, Y. et al. Bioaccessibility-corrected risk assessment of urban dietary methylmercury exposure via fish and rice consumption in China. *Sci. Total Environ.* **630**, 222–230 (2018).
23. Cui, W. et al. Occurrence of methylmercury in rice-based infant cereals and estimation of daily dietary intake of methylmercury for infants. *J. Agric. Food Chem.* **65**, 9569–9578 (2017).
24. Zhu, W. et al. Global observations and modeling of atmosphere–surface exchange of elemental mercury: a critical review. *Atmos. Chem. Phys.* **16**, 4451–4480 (2016).
25. Hsu-Kim, H., Kucharzyk, K. H., Zhang, T. & Deshusses, M. A. Mechanisms regulating mercury bioavailability for methylating microorganisms in the aquatic environment: a critical review. *Environ. Sci. Technol.* **47**, 2441–2456 (2013).
26. Bishop, K. et al. Recent advances in understanding and measurement of mercury in the environment: terrestrial Hg cycling. *Sci. Total Environ.* **721**, 137647 (2020).
27. Zhou, J., Obrist, D., Dastoor, A., Jiskra, M. & Ryjkov, A. Vegetation uptake of mercury and impacts on global cycling. *Nat. Rev. Earth Environ.* **2**, 269–284 (2021).
28. Obrist, D. et al. A review of global environmental mercury processes in response to human and natural perturbations: changes of emissions, climate, and land use. *Ambio* **47**, 116–140 (2018).
29. Zhang, T. & Hsu-Kim, H. Photolytic degradation of methylmercury enhanced by binding to natural organic ligands. *Nat. Geosci.* **3**, 473–476 (2010).
30. Luo, H., Cheng, Q. & Pan, X. Photochemical behaviors of mercury (Hg) species in aquatic systems: a systematic review on reaction process, mechanism, and influencing factor. *Sci. Total Environ.* **720**, 137540 (2020).
31. Gill, S. S. & Tuteja, N. Reactive oxygen species and antioxidant machinery in abiotic stress tolerance in crop plants. *Plant Physiol. Biochem.* **48**, 909–930 (2010).
32. Chen, T. & Fluhr, R. Singlet oxygen plays an essential role in the root's response to osmotic stress. *Plant Physiol.* **177**, 1717–1727 (2018).
33. Koh, E., Carmieli, R., Mor, A. & Fluhr, R. Singlet oxygen-induced membrane disruption and serpin–protease balance in vacuolar-driven cell death. *Plant Physiol.* **171**, 1616–1625 (2016).
34. Taverne, Y. J. et al. Reactive oxygen species: radical factors in the evolution of animal life: a molecular timescale from Earth's earliest history to the rise of complex life. *Bioessays* **40**, 1–9 (2018).
35. Sheng, F. et al. A new pathway of monomethylmercury photodegradation mediated by singlet oxygen on the interface of sediment soil and water. *Environ. Pollut.* **248**, 667–675 (2019).
36. Shapiro, A. M. & Chan, H. M. Characterization of demethylation of methylmercury in cultured astrocytes. *Chemosphere* **74**, 112–118 (2008).
37. Yasutake, A. & Hirayama, K. Evaluation of methylmercury biotransformation using rat liver slices. *Arch. Toxicol.* **75**, 400–406 (2001).
38. Suda, I., Totoki, S. & Takahashi, H. Degradation of methyl and ethyl mercury into inorganic mercury by oxygen free radical-producing systems: involvement of hydroxyl radical. *Arch. Toxicol.* **65**, 129–134 (1991).
39. Crump, K. S., Kjellström, T., Shipp, A. M., Silvers, A. & Stewart, A. Influence of prenatal mercury exposure upon scholastic and psychological test performance: benchmark analysis of a New Zealand cohort. *Risk Anal.* **18**, 701–713 (1998).
40. Grandjean, P. et al. Cognitive deficit in 7-year-old children with prenatal exposure to methylmercury. *Neurotoxicol. Teratol.* **19**, 417–428 (1997).
41. Myers, G. J. et al. Prenatal methylmercury exposure from ocean fish consumption in the Seychelles child development study. *Lancet* **361**, 1686–1692 (2003).
42. Rothenberg, S. E. et al. Stable mercury isotopes in polished rice (*Oryza sativa* L.) and hair from rice consumers. *Environ. Sci. Technol.* **51**, 6480–6488 (2017).
43. Salkever, D. S. Updated estimates of earnings benefits from reduced exposure of children to environmental lead. *Environ. Res.* **70**, 1–6 (1995).
44. Heckman, J. J., Stixrud, J. & Urzua, S. The effects of cognitive and noncognitive abilities on labor market outcomes and social behavior. *J. Labor. Econ.* **24**, 411–482 (2006).

45. Zhang, W. et al. Economic evaluation of health benefits of mercury emission controls for China and the neighboring countries in East Asia. *Energy Policy* **106**, 579–587 (2017).
46. Hasanuzzaman, M. et al. Reactive oxygen species and antioxidant defense in plants under abiotic stress: revisiting the crucial role of a universal defense regulator. *Antioxidants* **9**, 681 (2020).
47. Rothenberg, S. E. & Feng, X. Mercury cycling in a flooded rice paddy. *J. Geophys. Res. Biogeosci.* **117**, G03003 (2012).
48. Tang, W. et al. Increased methylmercury accumulation in rice after straw amendment. *Environ. Sci. Technol.* **53**, 6144–6153 (2019).
49. Lee, C. S. & Fisher, N. S. Microbial generation of elemental mercury from dissolved methylmercury in seawater. *Limnol. Oceanogr.* **64**, 679–693 (2019).
50. Mence Chaintreuil, C. et al. Photosynthetic bradyrhizobia are natural endophytes of the African wild rice *Oryza breviligulata*. *Appl. Environ. Microbiol.* **66**, 5437–5447 (2000).
51. Han, X., Li, Y., Li, D. & Liu, C. Role of free radicals/reactive oxygen species in MeHg photodegradation: importance of utilizing appropriate scavengers. *Environ. Sci. Technol.* **51**, 3784–3793 (2017).
52. Štrok, M., Hintelmann, H. & Dimock, B. Development of pre-concentration procedure for the determination of Hg isotope ratios in seawater samples. *Anal. Chim. Acta* **851**, 57–63 (2014).
53. Hintelmann, H. & Ogrinc, N. Determination of stable mercury isotopes by ICP/MS and their application in environmental studies. In *Biogeochemistry of Environmentally Important Trace Elements* 321–338 (ACS, 2003).
54. Krieger-Liszkay, A., Trösch, M. & Krupinska, K. Generation of reactive oxygen species in thylakoids from senescing flag leaves of the barley varieties Lomerit and Carina. *Planta* **241**, 1497–1508 (2015).
55. Ossola, R., Jönsson, O. M., Moor, K. & McNeill, K. Singlet oxygen quantum yields in environmental waters. *Chem. Rev.* **121**, 4100–4146 (2021).
56. Frisch, M. J. et al. Gaussian 16. (Gaussian, Inc., 2016).
57. Zhao, Y. & Truhlar, D. G. The M06 suite of density functionals for main group thermochemistry, thermochemical kinetics, noncovalent interactions, excited states, and transition elements: two new functionals and systematic testing of four M06-class functionals and 12 other functionals. *Theor. Chem. Acc.* **120**, 215–241 (2008).
58. Andrae, D., Iubermann, U. H., Dolg, M., Stoll, H. & Preub, H. Energy-adjusted ab initio pseudopotentials for the second and third row transition elements. *Theor. Chim. Acta* **77**, 123–141 (1990).
59. Marenich, A. V., Cramer, C. J. & Truhlar, D. G. Universal solvation model based on solute electron density and on a continuum model of the solvent defined by the bulk dielectric constant and atomic surface tensions. *J. Phys. Chem. B* **113**, 6378–6396 (2009).

Acknowledgements

The authors gratefully acknowledge L. Gan from Nanjing Agriculture University for the advice on endophytes. Y.G. is supported by National Natural Science Foundation of China (U2032201). W.T. appreciates the financial support from National Natural Science Foundation of China (42107223), Fundamental Research Funds for the Central Universities (021114380175) and Natural Science Foundation of Jiangsu Province (BK20190319). J.Z. is thankful for the support from National Natural Science Foundation of China (12222509). H.H. acknowledges the funding from the NSERC Discovery Grant Program (RGPIN-2018-05421). S.L. appreciates Golden Goose Research Grant Scheme (GGRG) (UMT/RMIC/2-2/25 Jld 5 (64), Vot 55191). A.J. and B.G. are supported by the Office of Biological and Environmental Research within the Office of Science of the US Department of Energy at Oak Ridge National Laboratory, which is managed by UT-Battelle, LLC, under contract number DE-AC05-00OR22725 with the US Department of Energy. H.R. gets support from National Natural Science Foundation of China (52388101).

Author contributions

H.Z., J.Z. and Y.G. led this project and designed all experiments. W.T. carried out the enriched isotope experiment under the supervision of H.H.; W.T., X.B., Y. Zhou, Y.Y., J.W. and S.L. conducted the crop experiment, rice growth stage experiment, Hg release experiment, homogenate experiment and quencher addition experiment under the supervisions of J.Z., Y.G. and H.Z.; W.T. estimated the avoided IQ decrements/economic benefits and Hg releases; L.N. helped conduct the sensitivity analysis, and C.L. conducted DFT calculations. W.T., H.Z. and C.S. led the manuscript writing and revision, and all coauthors participated in the writing and/or editing.

Competing interests

The authors declare no competing interests.

Additional information

Extended data is available for this paper at https://doi.org/10.1038/s43016-023-00910-x.

Supplementary information The online version contains supplementary material available at https://doi.org/10.1038/s43016-023-00910-x.

Correspondence and requests for materials should be addressed to Christian Sonne, Yuxi Gao, Jiating Zhao or Huan Zhong.

Peer review information *Nature Food* thanks Kevin Bishop, Xuejun Wang and Ping Li for their contribution to the peer review of this work.

[1]School of the Environment, Nanjing University, State Key Laboratory of Pollution Control and Resource Reuse, Nanjing, China. [2]Key Laboratory for Biomedical Effects of Nanomaterials and Nanosafety, Institute of High Energy Physics (IHEP), Chinese Academy of Sciences (CAS), Beijing, China. [3]University of Chinese Academy of Sciences, Beijing, China. [4]Department of Ecoscience, Arctic Research Centre, Aarhus University, Roskilde, Denmark. [5]Sustainability Cluster, School of Engineering, University of Petroleum and Energy Studies, Dehradun, India. [6]Higher Institution Centre of Excellence (HICoE), Institute of Tropical Aquaculture and Fisheries (AKUATROP), Universiti Malaysia Terengganu, Kuala Nerus, Malaysia. [7]Center for Global Health Research (CGHR), Saveetha Institute of Medical and Technical Sciences (SIMATS), Saveetha University, Chennai, India. [8]Department of Chemistry and School of the Environment, Trent University, Peterborough, Ontario, Canada. [9]Department of Physical and Environmental Sciences, University of

Toronto Scarborough, Scarborough, Ontario, Canada. [10]Environmental Sciences Division, Oak Ridge National Laboratory, Oak Ridge, TN, USA. [11]Faculty of Sciences and Technology, Civil Engineering Research and Innovation for Sustainability Center, University of Algarve, Faro, Portugal. [12]Key Laboratory of Soil Environment and Pollution Remediation, Institute of Soil Science, Chinese Academy of Sciences, Nanjing, China. [13]College of Life Science and Technology, Jinan University, Guangzhou, China. [14]State Key Laboratory of Pharmaceutical Biotechnology, School of Life Sciences, Nanjing University, Nanjing, China. [15]School of Architecture and Civil Engineering, Institute of Foundation Engineering, Water and Waste Management, Laboratory of Soil and Groundwater Management, University of Wuppertal, Wuppertal, Germany. [16]Tianjin Key Laboratory of Environmental Technology for Complex Trans-Media Pollution, College of Environmental Science and Engineering, Nankai University, Tianjin, China. [17]Key Laboratory of Geographic Information Science (Ministry of Education), School of Geographic Sciences, East China Normal University, Shanghai, China. [18]School of Atmospheric Sciences, Nanjing University, Nanjing, China. [19]State Key Joint Laboratory of Environmental Simulation and Pollution Control, School of Environment, Tsinghua University, Beijing, China. [20]State Environmental Protection Key Laboratory of Sources and Control of Air Pollution Complex, Beijing, China. [21]Korea Biochar Research Center, APRU Sustainable Waste Management Program and Division of Environmental Science and Ecological Engineering, Korea University, Seoul, Republic of Korea. [22]State Key Laboratory of Environmental Chemistry and Ecotoxicology, Research Center for Eco-Environmental Sciences, Chinese Academy of Sciences, Beijing, China. [23]State Key Laboratory of Radiation Medicine and Protection, Soochow University, Suzhou, China. [24]Department of Environmental Science, Zhejiang University, Hangzhou, China. [25]These authors contributed equally: Wenli Tang, Xu Bai, Yang Zhou. ✉e-mail: cs@ecos.au.dk; gaoyx@ihep.ac.cn; zhaojt@zju.edu.cn; zhonghuan@nju.edu.cn

https://doi.org/10.1038/s43016-023-00910-x

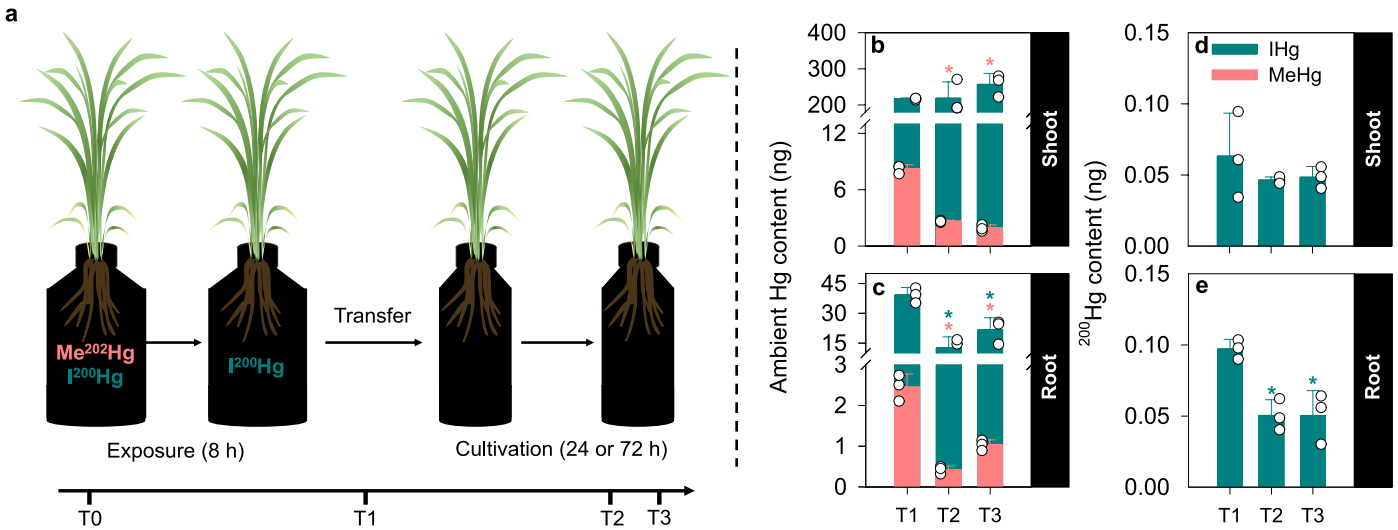

Extended Data Fig. 1 | The design of the enriched isotope experiment (a), and the contents of ambient Hg (b and c) and ^{200}Hg (d and e) in rice tissues. T0 refers to the time when exposure started ($Me^{202}Hg$ and $I^{200}Hg$ spiked into solutions); T1 refers to the time when exposure ended and plants were transferred (Only notable proportion of $I^{200}Hg$ remained in the solution, Supplementary Text 3); T2 and T3 refer to times when plants were further cultivated in Hg-free solution for 24 h (T2) and 72 h (T3), respectively. The contents of both THg and MeHg are calculated as the total mass (ng) to exclude the effect of biomass variability on concentration (that is, biodilution). For panels (b) to (e), data are shown as mean ± SD, n = 3 replicates. Asterisk (*) indicates significant ($p < 0.05$, one-way ANOVA) differences between two time points. The number of circles on the left and right margins of each bar correspond to three replicates of MeHg and THg, respectively.

https://doi.org/10.1038/s43016-023-00910-x

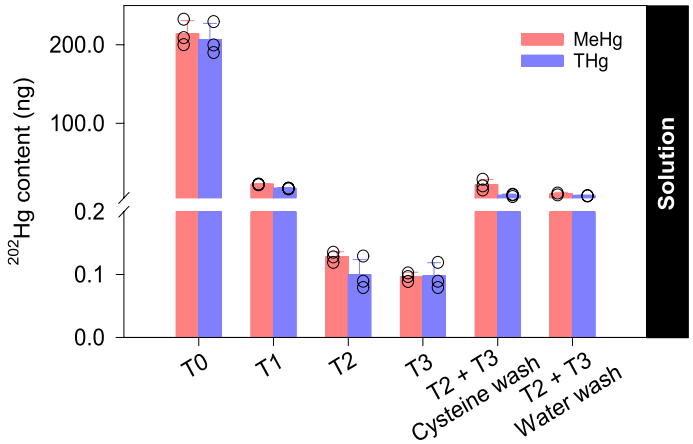

Extended Data Fig. 2 | Contents of T202Hg and Me202Hg in solutions of the enriched isotope experiment. T0 refers to the time when exposure started; T1 refers to the time when exposure ended and plants were transferred; T2 and T3 refer to times when plants were further cultivated in Hg-free solution for 24 h (T2) and 72 h (T3), respectively. Hg in cysteine wash and water wash includes the washing solutions for both roots and shoots. The contents of both THg and MeHg are calculated as the total mass (ng) in solution. Data are presented as Mean ± SD; for the bar of THg in T2+T3 cysteine wash, n = 4 replicates including a duplicate measurement; n = 2 for the bars of THg and MeHg in T2+T3 water wash due to experimental design; n = 3 replicates for the rest bars. Each replicate is depicted as a circle on the bar.

https://doi.org/10.1038/s43016-023-00910-x

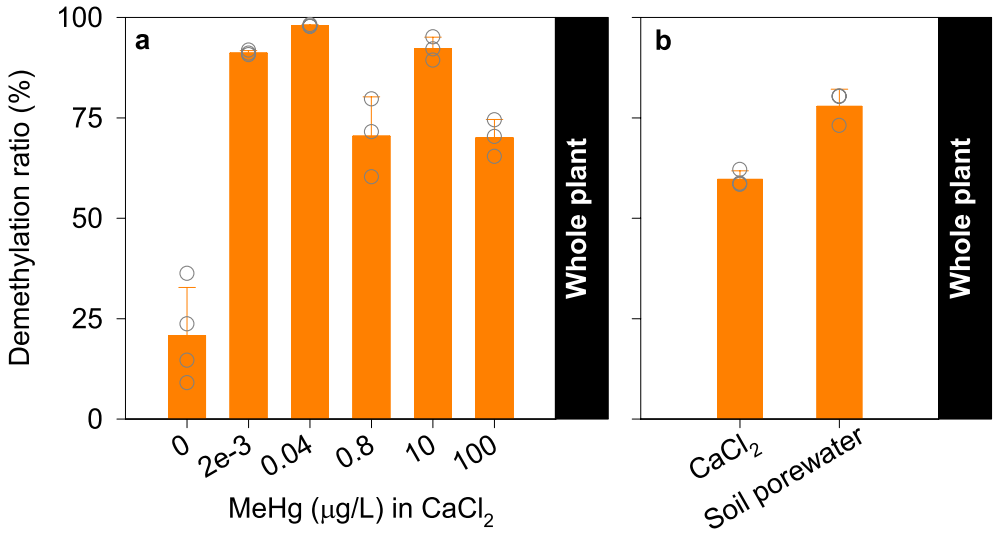

Extended Data Fig. 3 | The demethylation ratios (DRs) in rice plants after exposure to different concentrations of MeHg (a) and to 0.8 μg/L MeHg in different matrices (b). Note that experiments for panels (a) and (b) were conducted separately and thus the slightly lower DR in plants treated with $CaCl_2$ solution (b) compared with that in panel (a) is likely due to differences in the growth condition. Mean ± SD, n = 3 replicates. Noted that in panel a, DR at concentration of 0 was quantified separately and 4 replicates were set. Each replicate is depicted as a circle on the bar.

https://doi.org/10.1038/s43016-023-00910-x

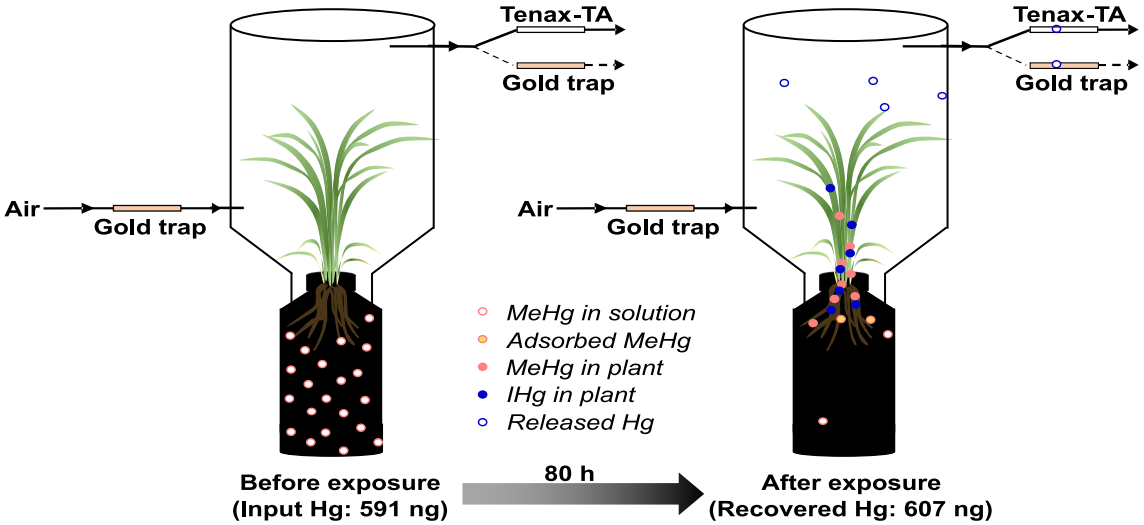

Extended Data Fig. 4 | Experimental design and Hg distribution after 80-h exposure in the Hg release experiment. It should be noted that this is a conceptual scheme, and details about Hg proportions and the recovery rate can be found in Supplementary Table 9.

https://doi.org/10.1038/s43016-023-00910-x

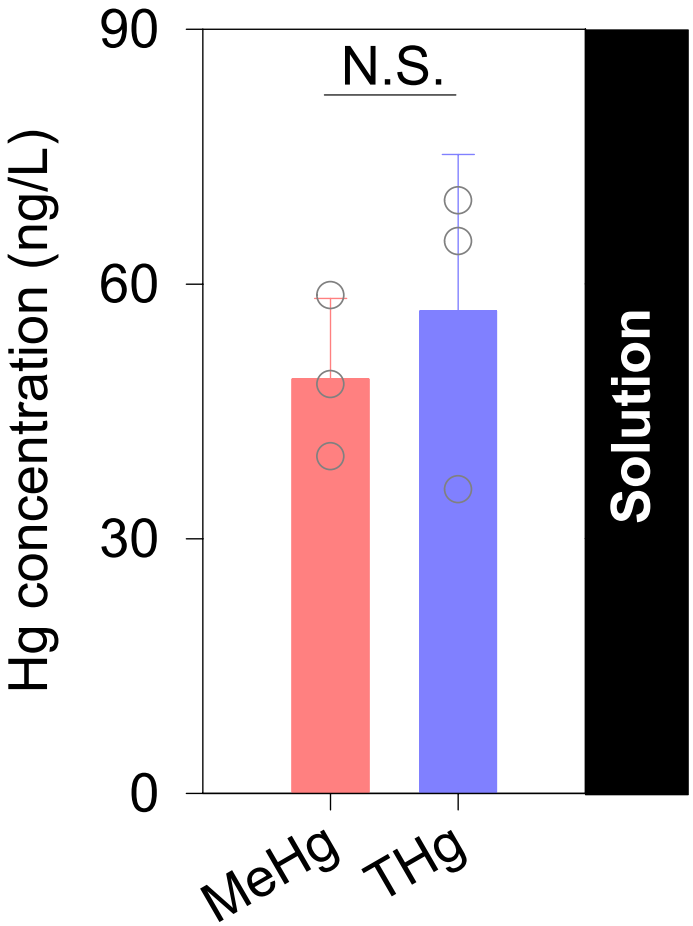

Extended Data Fig. 5 | The concentrations of MeHg and THg in solution after exposure in the Hg release experiment. N.S. indicates no significant difference between two parameters ($p > 0.05$, one-way ANOVA). Mean ± SD, n = 3 replicates. Each replicate is depicted as a circle on the bar.

https://doi.org/10.1038/s43016-023-00910-x

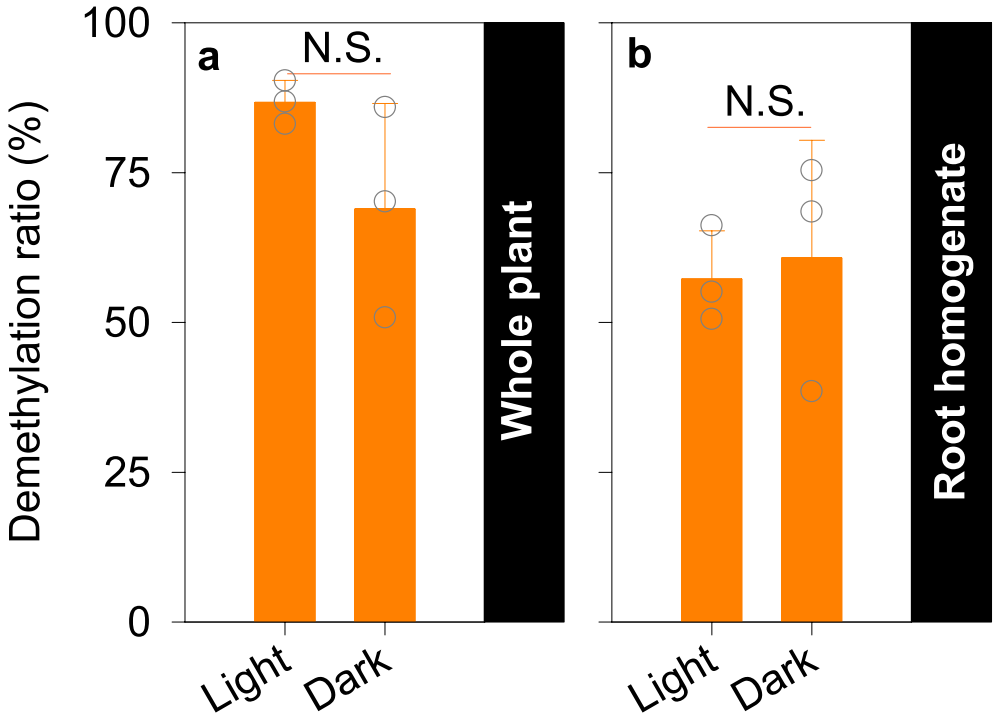

Extended Data Fig. 6 | The effect of light on MeHg demethylation in vivo (a) and in vitro (b). N.S. indicates no significant difference between two treatments ($p > 0.05$, one-way ANOVA). Mean ± SD, n = 3 replicates. Each replicate is depicted as a circle on the bar.

https://doi.org/10.1038/s43016-023-00910-x

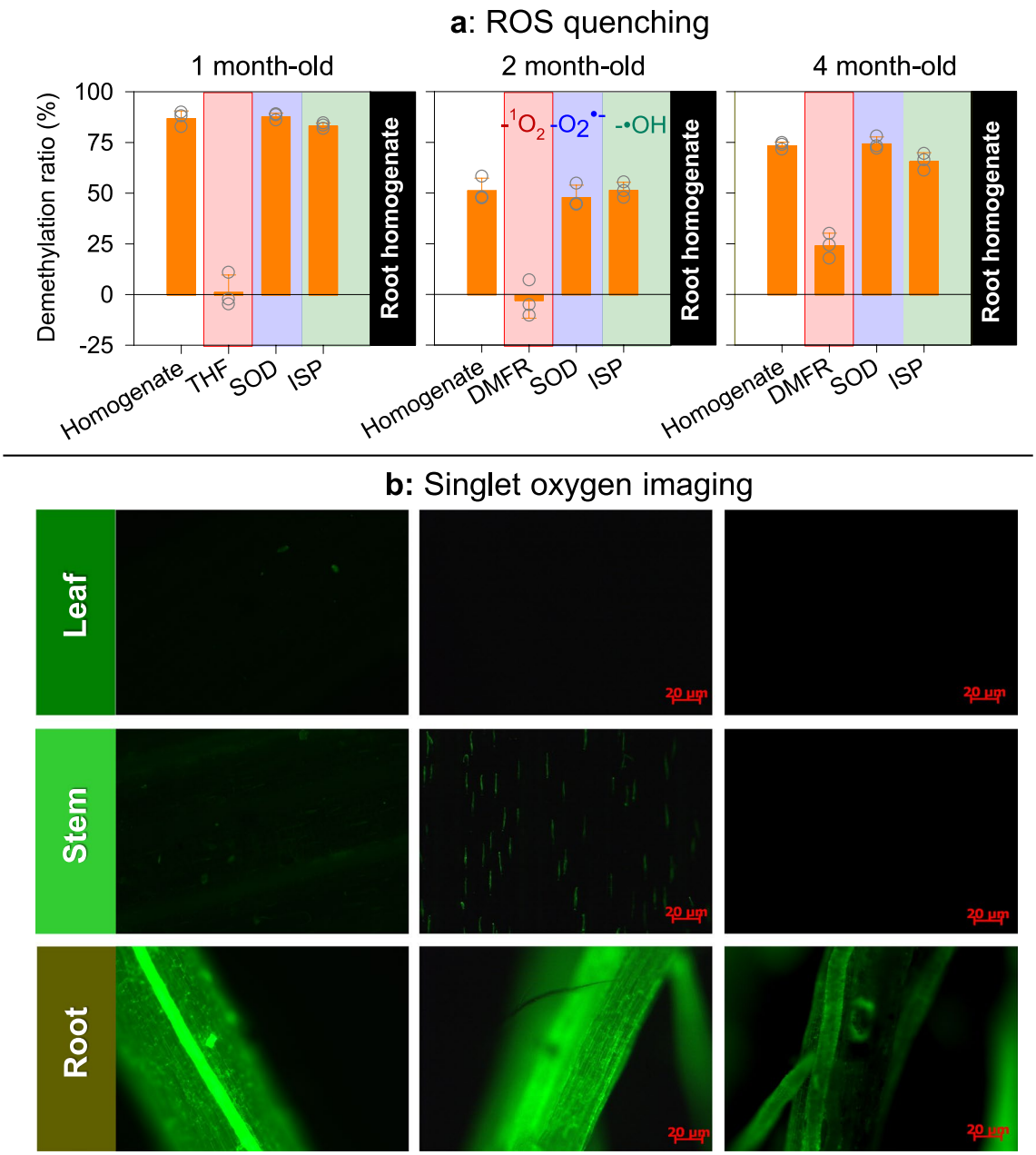

Extended Data Fig. 7 | The response of MeHg demethylation in root homogenates of rice plants to radical quencher additions (a) and the appearance of singlet oxygen from rice plants (1-, 2- and 4-month-old, left to right in panel b). THF instead of DMFR was used in 1-month-old plants to scavenge singlet oxygen since the type of quencher has only a minor effect on the DR. In panel (**a**), data are shown as mean ± SD, n = 3 replicates. Each replicate is depicted as circle on the bar. Original photos in panel b are provided as Source Data.

https://doi.org/10.1038/s43016-023-00910-x

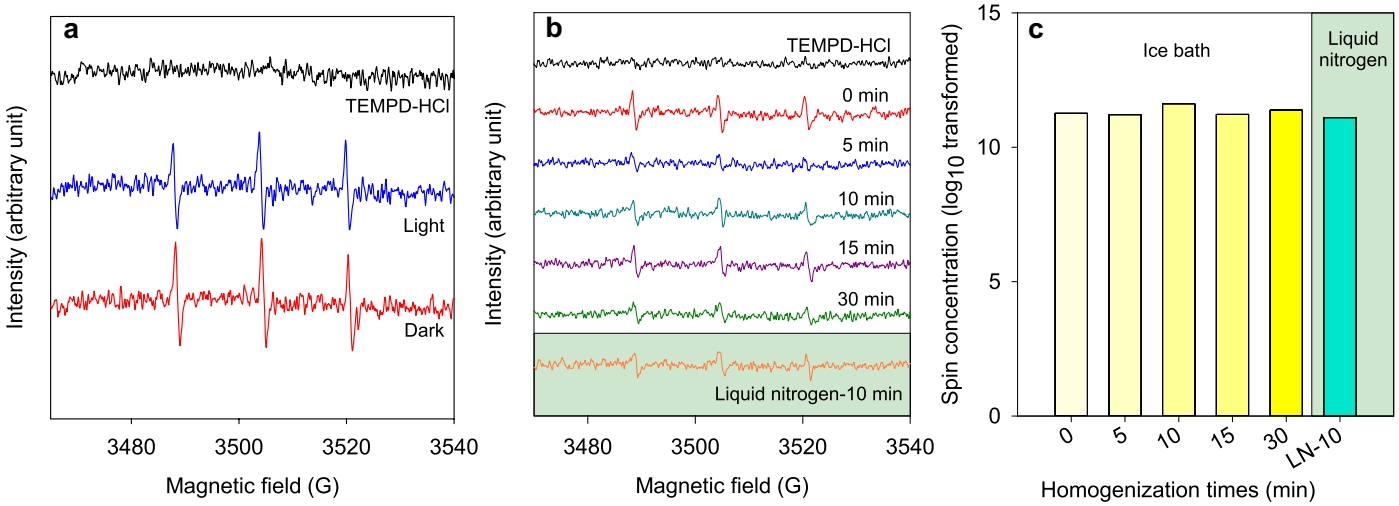

Extended Data Fig. 8 | Lines of evidence supporting the feasibility of using homogenates to detect the production of singlet oxygen. The EPR signal of singlet oxygen in supernatant fraction (< 0.22 μm) under the light or dark condition (**a**), and its signal (**b**) and spin concentrations in homogenates with different degrees of homogenization (**c**).

https://doi.org/10.1038/s43016-023-00910-x

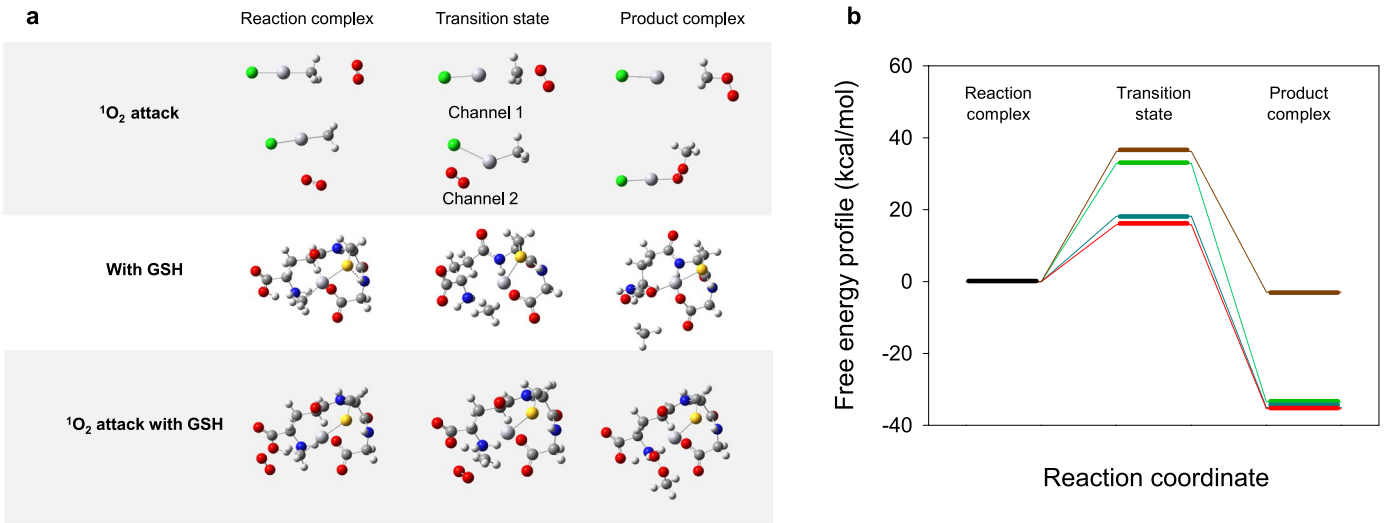

Extended Data Fig. 9 | Theoretic evidence supporting MeHg demethylation by singlet oxygen. The optimized geometries for the reactants, transition states and products for reactions of Hg-C bond cleavage in MeHg by the attack of singlet oxygen, or Hg-C bond cleavage in MeHg-GSH in the presence/absence of the attack of singlet oxygen (**a**) and Gibbs free-energy profiles of Hg-C bond cleavages in all reaction systems (**b**).

https://doi.org/10.1038/s43016-023-00910-x

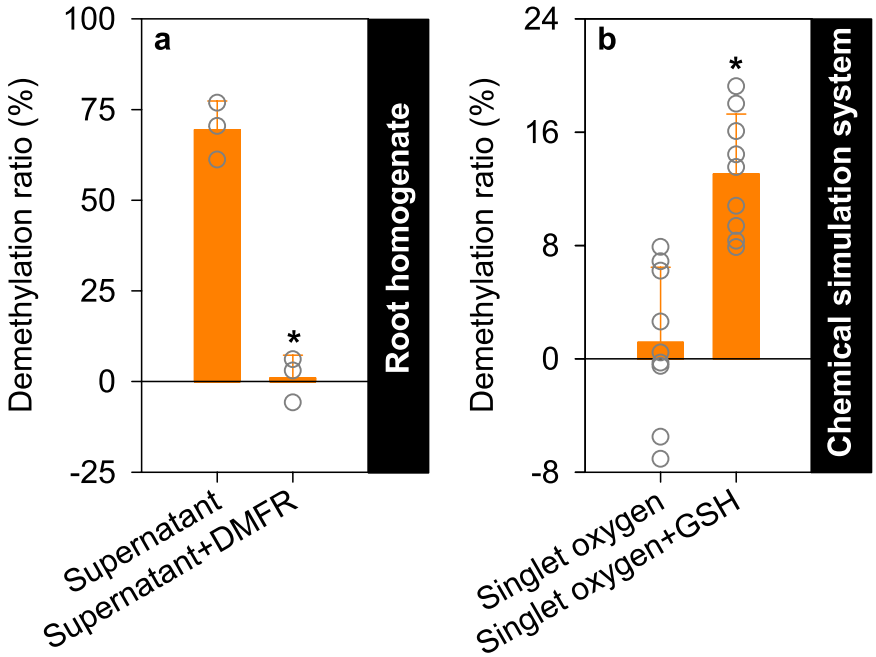

Extended Data Fig. 10 | The demethylation ratio of MeHg in the supernatant of root homogenate (< 0.22 μm fraction) without or with singlet oxygen quenched (a) and in singlet oxygen-generating chemical system in the absence or presence of GSH (b). In (**a**), data are presented as mean ± SD, n = 3 replicates. In (**b**), this experiment was repeated 3 times, and 3 replicates were set each time; thus, data are depicted as mean ± SD, n = 9 replicates. Each replicate is depicted as a circle on the bar.

nature portfolio

Corresponding author(s): Christine Sonne, Yuxi Gao, Jiating Zhao, Huan Zhong

Last updated by author(s): Nov. 29, 2023

Reporting Summary

Nature Portfolio wishes to improve the reproducibility of the work that we publish. This form provides structure for consistency and transparency in reporting. For further information on Nature Portfolio policies, see our Editorial Policies and the Editorial Policy Checklist.

Statistics

For all statistical analyses, confirm that the following items are present in the figure legend, table legend, main text, or Methods section.

n/a	Confirmed
☐	☒ The exact sample size (*n*) for each experimental group/condition, given as a discrete number and unit of measurement
☐	☒ A statement on whether measurements were taken from distinct samples or whether the same sample was measured repeatedly
☐	☒ The statistical test(s) used AND whether they are one- or two-sided *Only common tests should be described solely by name; describe more complex techniques in the Methods section.*
☐	☒ A description of all covariates tested
☐	☒ A description of any assumptions or corrections, such as tests of normality and adjustment for multiple comparisons
☐	☒ A full description of the statistical parameters including central tendency (e.g. means) or other basic estimates (e.g. regression coefficient) AND variation (e.g. standard deviation) or associated estimates of uncertainty (e.g. confidence intervals)
☐	☒ For null hypothesis testing, the test statistic (e.g. *F*, *t*, *r*) with confidence intervals, effect sizes, degrees of freedom and *P* value noted *Give P values as exact values whenever suitable.*
☒	☐ For Bayesian analysis, information on the choice of priors and Markov chain Monte Carlo settings
☒	☐ For hierarchical and complex designs, identification of the appropriate level for tests and full reporting of outcomes
☒	☐ Estimates of effect sizes (e.g. Cohen's *d*, Pearson's *r*), indicating how they were calculated

Our web collection on statistics for biologists contains articles on many of the points above.

Software and code

Policy information about availability of computer code

Data collection	No software was used for data collection.
Data analysis	Gaussian 16. Gaussian, Inc., Wallingford CT; PASW Statistics 18.0; Sigmaplot 14.0; Microsoft Office Home and Student 2019; and ArcMap 10.8.

For manuscripts utilizing custom algorithms or software that are central to the research but not yet described in published literature, software must be made available to editors and reviewers. We strongly encourage code deposition in a community repository (e.g. GitHub). See the Nature Portfolio guidelines for submitting code & software for further information.

Data

Policy information about availability of data

All manuscripts must include a data availability statement. This statement should provide the following information, where applicable:

- Accession codes, unique identifiers, or web links for publicly available datasets
- A description of any restrictions on data availability
- For clinical datasets or third party data, please ensure that the statement adheres to our policy

All the data supporting the findings are included in the main text, Supplementary Information, and the Source Data. The databases used in this study are FAO ((http://www.fao/fao.org/faostat/#en/#data/CC), World Rice Statistics (http://ricestat.irri.org:8080/wrs), World Bank (http://data.worldbank.org/indicator/NY.GDP.PCAP.PP.CD and http://data.worldbank.org/indicator/NY.GDP.PCAP.KD.ZG), World Population Perspective 2019 (https://population.un.org/wpp/), and Natural Earth (https://www.naturalearthdata.com/downloads/10m-cultural-vectors/).

Research involving human participants, their data, or biological material

Policy information about studies with human participants or human data. See also policy information about sex, gender (identity/presentation), and sexual orientation and race, ethnicity and racism.

Reporting on sex and gender	Not applicable.
Reporting on race, ethnicity, or other socially relevant groupings	Not applicable.
Population characteristics	Not applicable.
Recruitment	Not applicable.
Ethics oversight	Not applicable.

Note that full information on the approval of the study protocol must also be provided in the manuscript.

Field-specific reporting

Please select the one below that is the best fit for your research. If you are not sure, read the appropriate sections before making your selection.

☐ Life sciences ☐ Behavioural & social sciences ☒ Ecological, evolutionary & environmental sciences

For a reference copy of the document with all sections, see nature.com/documents/nr-reporting-summary-flat.pdf

Ecological, evolutionary & environmental sciences study design

All studies must disclose on these points even when the disclosure is negative.

Study description	This study investigates transformations of methylmercury within crop plants, the underlying mechanisms, as well as the protective effects of these processes on human health.
Research sample	A total of seven rice varieties, i.e., Wufeng, Liangyou900, Xiangliangyou900, Akitakomati, Yueguang, Jingliangyouhuazhan and Jingdao, were used in this study to explore the in vivo demethylation. These varieties were chosen since they are commonly planted in China. Eight kinds of crop plants, i.e., rice, wheat, maize, barley, rye, peanut, soybean and cabbage were used to explore methylmercury demethylation in plants considering these are common crops according to the planting area worldwide (based on the FAO database).
Sampling strategy	Crop plants (described above) were cultured hydroponically. 1) in vivo experiments: after the experimental treatment, e.g., exposing plants to methylmercury, all plants were separated into shoots and roots. Then, the tissues were washed sequentially with cysteine solution and deionized water, oven dried to constant weight and ground for Hg analyses. Generally, 3 replicates, each with 5 individual plants, were used for each treatment. The number of replicates were decided considering the individual differences of plants. 2) in vitro experiments: tissues were homogenized in ice bath, spiked with methylmercury, incubated for 5 days, and determined for methylmercury concentrations. Three replicates were used for each treatment, which are sufficient to ensure relatively low variability.
Data collection	Experimental data: Data were obtained from readings of instruments (e.g., Hg analyzer) and recorded in excel files by operators (e.g., Wenli Tang, and Yang Zhou). Literature data: Data were retrieved from published literatures and websites of FAO, the World Bank, etc., by Wenli Tang.
Timing and spatial scale	Not applicable.
Data exclusions	No data were excluded.
Reproducibility	Key experiments were repeated by different persons and the results (e.g., demethylation ratios) are consistent.
Randomization	Monte Carlo simulation is used to estimate the uncertainty of avoided IQ decrement and economic benefits. A total of 100,000 iterations are needed to achieve the stabilization of the percentiles with deviations of less than 5%.
Blinding	Not applicable as this is an observational study.

Did the study involve field work? ☐ Yes ☒ No

Reporting for specific materials, systems and methods

We require information from authors about some types of materials, experimental systems and methods used in many studies. Here, indicate whether each material, system or method listed is relevant to your study. If you are not sure if a list item applies to your research, read the appropriate section before selecting a response.

Materials & experimental systems

n/a	Involved in the study
☒	☐ Antibodies
☒	☐ Eukaryotic cell lines
☒	☐ Palaeontology and archaeology
☒	☐ Animals and other organisms
☒	☐ Clinical data
☒	☐ Dual use research of concern
☐	☒ Plants

Methods

n/a	Involved in the study
☒	☐ ChIP-seq
☒	☐ Flow cytometry
☒	☐ MRI-based neuroimaging

Dual use research of concern

Policy information about dual use research of concern

Hazards

Could the accidental, deliberate or reckless misuse of agents or technologies generated in the work, or the application of information presented in the manuscript, pose a threat to:

No	Yes
☒	☐ Public health
☒	☐ National security
☒	☐ Crops and/or livestock
☒	☐ Ecosystems
☒	☐ Any other significant area

Experiments of concern

Does the work involve any of these experiments of concern:

No	Yes
☒	☐ Demonstrate how to render a vaccine ineffective
☒	☐ Confer resistance to therapeutically useful antibiotics or antiviral agents
☒	☐ Enhance the virulence of a pathogen or render a nonpathogen virulent
☒	☐ Increase transmissibility of a pathogen
☒	☐ Alter the host range of a pathogen
☒	☐ Enable evasion of diagnostic/detection modalities
☒	☐ Enable the weaponization of a biological agent or toxin
☒	☐ Any other potentially harmful combination of experiments and agents